



Synthesis, characterization of 2-(bis-dibutylcarbamoylmethyl-amino)-*N*, *N*-dibutyl-acetamide (L) lanthanide picrate complexes (Ln = Nd, Eu, Tb) and the crystal structure of [Tb(pic)₃L]

Nan Yang^a, Jiangrong Zheng^a, Weisheng Liu^{a,*}, Ning Tang^a, Kaibei Yu^b

^aCollege of Chemistry and Chemical Engineering, Lanzhou University, Lanzhou 730000, China

^bChengdu Center of Analysis and Measurement, Academia Sinica, Chengdu 610041, China

Received 15 January 2003; revised 27 May 2003; accepted 30 May 2003

Abstract

Solid complexes of lanthanide picrate with the ligand 2-(bis-dibutylcarbamoylmethyl-amino)-*N*, *N*-dibutyl-acetamide (L), [Ln(pic)₃L] (Ln = Nd, Eu, Tb), have been prepared and characterized by elemental analysis, conductivity measurements, DTA and TGA analysis, IR and ¹H NMR spectra. For the terbium complex, X-ray measurements show that Tb(III) ion is 9-coordinated by three oxygen atoms and one nitrogen atom of L and five oxygen atoms of picrate groups. Molecule B has a clockwise structure due to the screw coordination arrangement of the tripod-type ligand.

© 2003 Elsevier B.V. All rights reserved.

Keywords: Lanthanide picrate; Complex; Tripod-type; Crystal structure; Cavity-like structure

1. Introduction

Amide-base tripod-type compounds have been widely studied in the extraction of lanthanide or some actinide ions, and in ion-selective electrodes [1–5]. The tripod-type ligands containing amide groups possess suitable molecular structure: a chain with flexible terminal groups. Therefore, they are excellent reagents for activating ion-selective electrodes and extracts of rare earth ions. Rare earth

complexes and their extraction studies of these types of compounds have been reported, among which 2-{2-[bis-(2-diethylcarbamoylmethoxy-ethyl)-amino]-ethoxy}-*N*,*N*-diethyl-acetamide shows a high extractability to lanthanide. This extractability mostly depends on cavity-like coordination structure and terminal group effects [6–8]. As a subsequent study of such ligands, in order to design better extractors and further explore the relationship between structure and extractability, we give here the synthesis, characterization of 2-(bis-dibutylcarbamoylmethyl-amino)-*N*, *N*-dibutyl-acetamide (L) lanthanide picrate complexes [Ln(pic)₃L] (Ln = Nd, Eu, Tb), and the crystal structure of [Tb(pic)₃L].

* Corresponding author. Tel.: +86-9318911809; fax: +86-9318912582.

E-mail address: liuws@lzu.edu.cn (W. Liu).

2. Experimental

2.1. Materials

The lanthanide picrate [9] and L [10] were prepared according to literature methods. All commercially available chemicals were of reagent grade and were used without further purification.

2.2. Synthesis of ligand

Scheme 1 shows the synthesis of ligand L. Oxalyl chloride (15.0 ml) was added dropwise to the mixture of (bis-carboxymethyl-amino)-acetic acid (1.5 g, 7.85 mmol, in 20 ml benzene) with one drop of DMF as catalyst. After the mixture had been stirred under 30 °C for 6 h, the benzene and extra oxalyl chloride were removed by decompress distillation under 50 °C. Dibutyl-amine (6.1 g, 47.29 mmol, in 30 ml benzene) was added and the mixture was heated to 40 °C. After being stirred for about 8 h, the precipitated solid was filtered, and the solvent was removed by decompress distillation. The crude product was chromatographed on silica gel (petroleum/CH₃COOC₂H₅, 5:1 (v/v)) to afford pure product as brown oil in 50% yield.

2.3. General preparation of the complexes

A solution of L (0.2 mmol, in 10 ml of ethanol) was added dropwise to a solution of lanthanide picrate (0.2 mmol, in 5 ml of ethanol). The mixture was stirred at room temperature for 8 h. The yellowish

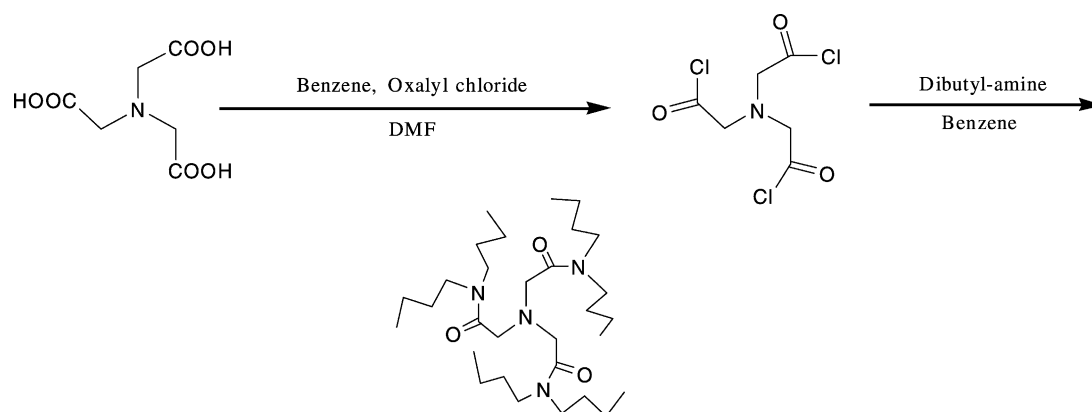
precipitated solid complex was filtered, washed with ethanol three times and dried in vacuo over P₄O₁₀ for 48 h. Single crystal of the terbium picrate complex grew from methanol/acetone by slow evaporation at room temperature. After about a month, transparent yellowish crystals formed from the solution.

2.4. Chemical and physical measurements

The metal ions were determined by EDTA titration using xylenol orange as an indicator. C, N and H were determined using an Elementar Vario EL. IR spectra were recorded on a Nicolet AVATAR 360 FTIR instrument using KBr discs in the 400–4000 cm⁻¹ region, ¹H NMR spectra were measured on a Bruker AC 200 spectrometer in CDCl₃ solution with TMS as internal standard. Conductivity measurements were carried out with a DDSJ-308 type conductivity bridge using 1 × 10⁻³ mol/l solutions in acetone at 25 °C.

2.5. X-ray crystallography

For the terbium complex, X-ray measurements were performed on a P4 four-circle diffractometer with graphite monochromatized Mo K_α radiation at 291(2) K using the ω/2θ scan mode. Lorentz and polarization corrections were applied, and empirical absorption correction was made. A summary of crystallographic data and details of the structure refinements are listed in Table 1. The structure was solved by direct methods and refined by full-matrix least-square techniques with all non-hydrogen atoms treated anisotropically. All calculations were



Scheme 1. The Synthesis of ligand L.

Table 1
Crystal data and structure refinement for the complex [Tb(pic)₃L]

Empirical formula	C ₄₈ H ₆₆ N ₁₃ O ₂₄ Tb
Temperature (K)	291(2)
Crystal color	Yellow
Crystal size (mm ³)	0.56 × 0.48 × 0.46
Formula weight	1368.06
Crystal system	Monoclinic
Space group	<i>P</i> 2 ₁ / <i>c</i>
Unit cell dimension	
<i>a</i> (Å)	23.123(5)
<i>b</i> (Å)	19.794(4)
<i>c</i> (Å)	29.112(6)
α (degree)	90
β (degree)	112.61(2)
γ (degree)	90
<i>V</i> (Å ³)	12300(4)
<i>Z</i>	8
Density (calculated, g/cm ³)	1.477
<i>F</i> (000)	5616
Radiation, graphite monochromatized, λ (Å)	0.71073
μ (Mo K α) (cm ⁻¹)	5.67
Reflections collected	23,676
Independent reflections	21,662
θ range for data collection	1.52–25.00
Index range	0 ≤ <i>h</i> ≤ 27, 0 ≤ <i>k</i> ≤ 23, -34 ≤ <i>l</i> ≤ 31
Goodness-of-fit on <i>F</i> ²	0.777
<i>R</i> [<i>I</i> > 2 σ (<i>I</i>)]	<i>R</i> ₁ = 0.0541, <i>wR</i> ₂ = 0.1116 ^a
<i>R</i> (all data)	<i>R</i> ₁ = 0.1625, <i>wR</i> ₂ = 0.1377 ^a
Largest difference peak and hole [e Å ⁻³]	0.539, -1.065

$$^a w = 1/[\sigma^2(F_o)^2 + (0.0337p)^2] \text{ where } p = (F_o^2 + F_c^2)/3.$$

performed on an Eclipse S/140 computer with the program package SHELXTL [11] version 5.10.

3. Results and discussion

3.1. Properties of the complexes

Analytical data for the complex conform to a 1:3:1 metal-to-picrate-to-L stoichiometry [Ln(pic)₃L] (Table 2). All complexes are soluble in DMSO, DMF, THF, CHCl₃, CH₃CN, methanol and acetone, and sparingly soluble in benzene, Et₂O and cyclohexane. Conductivity measurements for these complexes in acetone solution (Table 3)

Table 2
Analytical data for the complexes (calculate values in parentheses)

Complex	Analysis (%)			
	C	H	N	Ln
Nd(pic) ₃ L	42.77(42.60)	5.09(5.08)	12.92(13.45)	10.13(10.67)
Eu(pic) ₃ L	41.96(42.36)	4.53(4.89)	13.16(13.38)	11.35(11.17)
Tb(pic) ₃ L	41.88(42.14)	5.10(4.86)	13.40(13.31)	11.24(11.63)

indicate that all the three picrate groups coordinate to Ln(III) in each complex [12].

3.2. ¹H NMR spectra

The spectrum of the ligand exhibits four multiples at 0.92, 1.31, 1.50 and 3.28 ppm assigned to -CH₃, CH₃-CH₂-, CH₃-CH₂-CH₂- and -CH₂-N, and one single peak at 3.67 ppm to N-CH₂-C=O protons, respectively (Table 4).

3.3. IR spectra

Free L shows band at 1642 cm⁻¹ which may be assigned to ν (C=O). In the IR spectra of the lanthanum complexes, the disappearances of free picrate acid ν (O-H) characteristic frequency (3445 cm⁻¹) indicate that the O-H groups take part in coordination and the hydrogen atoms are substituted by lanthanide ions.

In the IR spectra of complexes, the bands of ν (C=O) of free L shift about 30 cm⁻¹ towards lower wave number, indicating the C=O groups take part in coordination to the metal ions. The larger band shifts for ν (C-O) (62 cm⁻¹) in the spectra of complexes suggest that the Ln-O (phenol) bonds are stronger than Ln-O (carbonyl) ones [13]. Furthermore, the characteristic frequencies (1342, 1555 cm⁻¹) of free

Table 3
Conductivity of complexes (concentration of complexes: 1 × 10⁻³ mol/l, temperature: 25 °C)

Compounds	Conductivity (Λm)
Acetone	0.7 S cm ² mol ⁻¹
Nd(pic) ₃ L	48.2 S cm ² mol ⁻¹
Eu(pic) ₃ L	47.3 S cm ² mol ⁻¹
Tb(pic) ₃ L	45.7 S cm ² mol ⁻¹

Table 4
The ^1H NMR spectrum of ligand (ppm)

Compound	$\delta\text{-CH}_3$	$\delta\text{CH}_3\text{-CH}_2\text{-}$	$\delta\text{CH}_3\text{-CH}_2\text{-CH}_2\text{-}$	$\delta\text{-N-CH}_2\text{-}$	$\delta\text{-N-CH}_2\text{-C=O}$
L	0.92	1.31	1.50	3.28	3.67

Table 5
The relevant characteristic IR bands (cm^{-1})

	$\nu(\text{C=O})$	$\nu(\text{O-H})$	$\nu(\text{C-O})$	$\nu_{\text{as}}(-\text{NO}_2)$	$\nu_{\text{s}}(-\text{NO}_2)$
Ligand (L)	1642				
Picrate acid		3445	1213	1555	1342
Nd(pic) $_3$ L	1611		1275	1574, 1545	1360, 1324
Eu(pic) $_3$ L	1613		1275	1576, 1544	1362, 1324
Tb(pic) $_3$ L	1613		1275	1576, 1545	1362, 1325

picrate were divided into two double peaks (about 1362, 1325 and 1576, 1545 cm^{-1} , respectively), indicating that the picrate groups coordinate to the metal ions as bidentate ligands [14] (Table 5).

3.4. DTA and TGA analysis

In the DTA and TGA spectra of complex [Tb(pic) $_3$ L], a heat-absorb peak appeared at about 80 °C without any loss of weight indicating that the melting point of the complex is 80 °C. As the temperature rising, the heat-emission bands appeared, beginning at 250 °C, with successive weight loss. At the 500 °C, the complex completely convert into Tb $_4$ O $_7$ and the weight become stable (Fig. 1). The experimental total weight-loss value (85.67%) is similar to the calculated one (86.25%).

The DTA and TGA spectra of [Nd(pic) $_3$ L] and [Eu(pic) $_3$ L] are similar to that of [Tb(pic) $_3$ L]. All the complexes begin to lose weight at about 250 °C, and completely convert into oxide (Nd $_2$ O $_3$, Eu $_2$ O $_3$ and Tb $_4$ O $_7$) after 500 °C. The differences among them are the melting point and the total weight-loss value. For complex [Nd(pic) $_3$ L], the melting point is 69 °C and the experimental total weight-loss value is 86.61% (87.56%, calculated). The melting point for complex [Eu(pic) $_3$ L] is 73 °C and the experimental total weight-loss value is 86.79% (87.06%, calculated).

3.5. X-ray crystal structure

Fig. 2 shows the structure and the atomic numbering schemes of the terbium complex. Fig. 3 shows the stacking pattern along y-axis in the unit cell. Selected bond lengths and angles are given in Table 6.

In the complex, L acts as a tetradentate ligand; two bidentate and one-unidentate picrate groups to give 9-coordination occupy the remaining coordination sites. Upon coordination, L gives two different arrangements around Tb(III) ions. In structure A, the torsion angles of Tb(1)–N(1)–C(1)–C(2), Tb(1)–N(1)–C(11)–C(12)

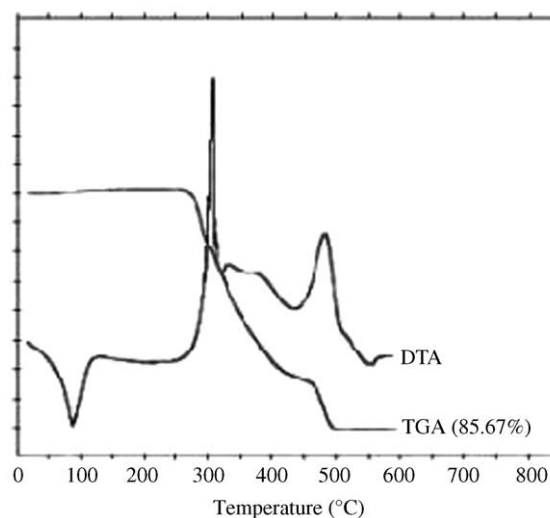


Fig. 1. The DTA and TGA spectra of [Tb(pic) $_3$ L].

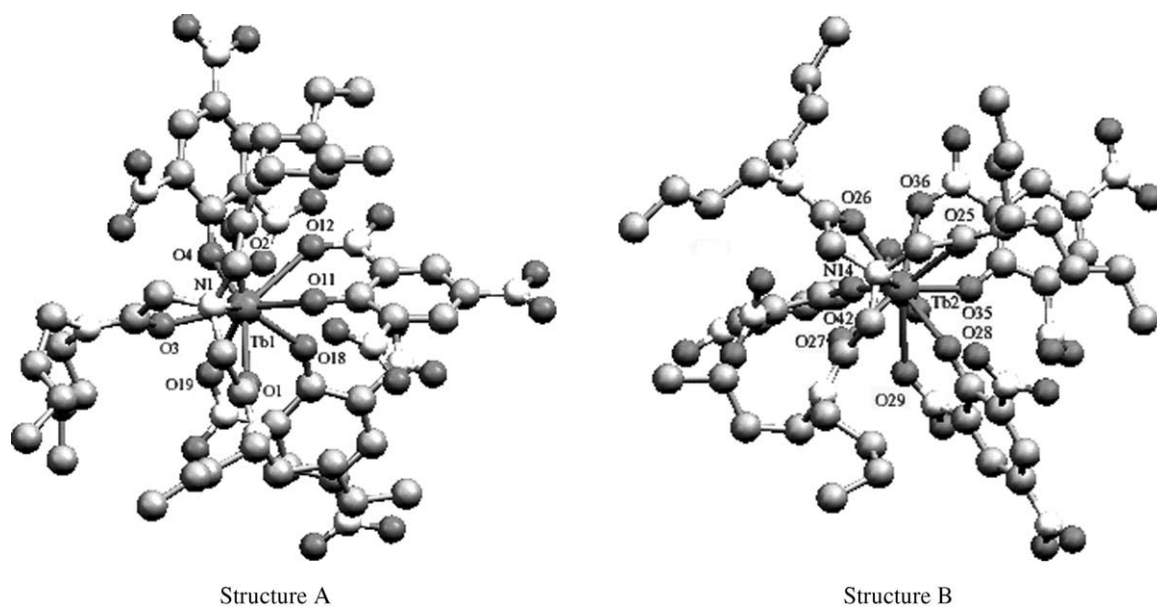


Fig. 2. The structure of $[\text{Tb}(\text{pic})_3\text{L}]$, showing 50% thermal ellipsoids. Hydrogen atoms have been omitted for clarity.

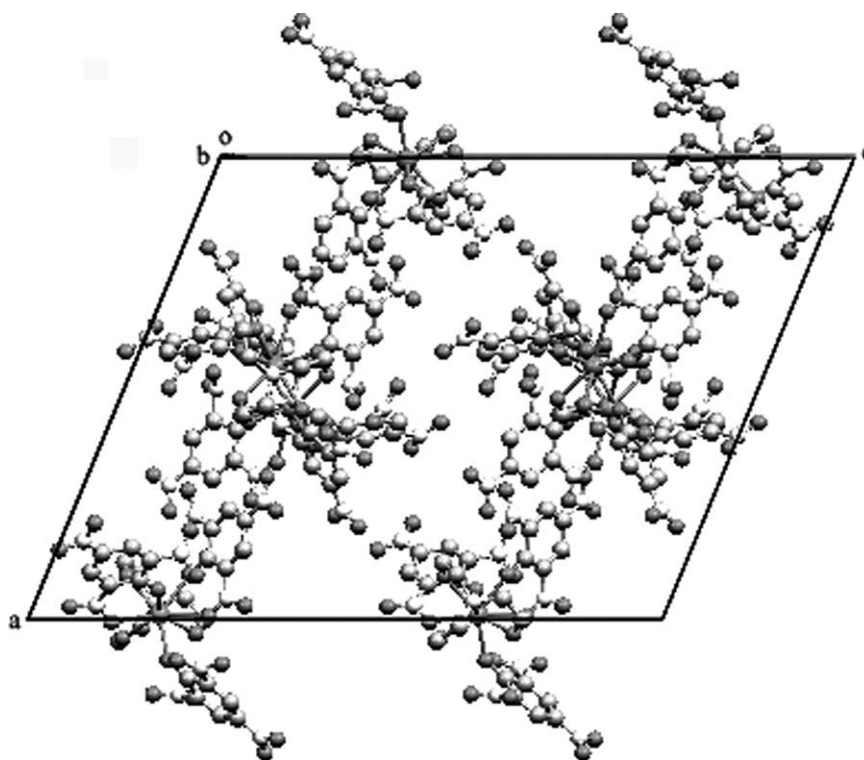


Fig. 3. The structure of $[\text{Tb}(\text{pic})_3\text{L}]$ in the unit cell. Some atoms have been omitted for clarity.

Table 6
Selected bond lengths (Å) and bond angles (degree) for [Tb(pic)₃L]

Tb(1)–O(1)	2.359(6)	Tb(2)–O(25)	2.320(6)
Tb(1)–O(2)	2.387(5)	Tb(2)–O(26)	2.296(6)
Tb(1)–O(3)	2.327(6)	Tb(2)–O(27)	2.380(6)
Tb(1)–O(4)	2.274(5)	Tb(2)–O(28)	2.359(5)
Tb(1)–O(11)	2.319(5)	Tb(2)–O(29)	2.591(7)
Tb(1)–O(12)	2.580(6)	Tb(2)–O(35)	2.292(6)
Tb(1)–O(18)	2.325(5)	Tb(2)–O(36)	2.681(7)
Tb(1)–O(19)	2.630(6)	Tb(2)–O(42)	2.240(6)
Tb(1)–N(1)	2.686(6)	Tb(2)–N(14)	2.695(7)
Tb(1)–N(1)–C(1)	111.4(4)	Tb(2)–N(14)–C(49)	110.9(5)
Tb(1)–N(1)–C(11)	108.6(4)	Tb(2)–N(14)–C(59)	108.8(5)
Tb(1)–N(1)–C(21)	107.5(4)	Tb(2)–N(14)–C(69)	106.4(5)
N(1)–C(1)–C(2)	112.8(7)	N(14)–C(49)–C(50)	112.1(8)
N(1)–C(11)–C(12)	107.2(7)	N(14)–C(59)–C(60)	109.8(7)
N(1)–C(21)–C(22)	110.8(7)	N(14)–C(69)–C(70)	107.8(8)

and Tb(1)–N(1)–C(21)–C(22) are -5.79 , 35.65 and 35.37° , respectively, while in structure B, the torsion angles of Tb(2)–N(14)–C(49)–C(50), Tb(2)–N(14)–C(59)–C(60) and Tb(2)–N(14)–C(69)–C(70) are -4.28 , -27.52 and -40.01° , respectively, which induce a chiral structure (Fig. 4).

In structure A, the value of the Tb–N distance (2.686 Å) is longer than the average Tb–O (C=O) bond distance (2.358 Å), indicating that Tb–O (C=O) bond is stronger than the Tb–N one. The same situation occurs in structure B, where the average

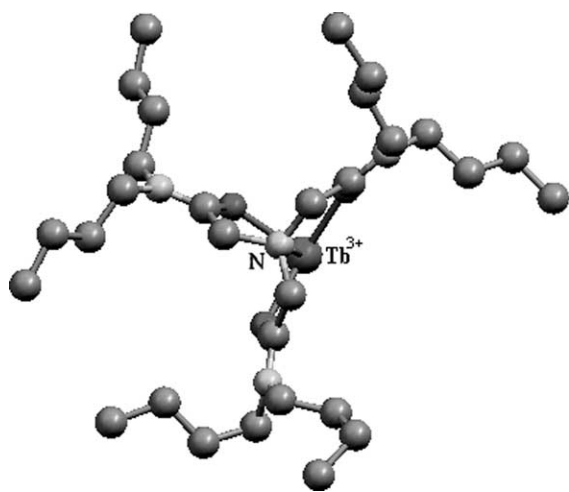


Fig. 4. L of molecule B shows a clockwise arrangement looking from N to Tb(III).

distance between Tb(2) atom and oxygen atoms (C=O) is 2.332 Å and the distance between Tb(2) and apex nitrogen atom is 2.695 Å.

In conclusion, amide-base tripod-type ligand L can form stable solid complexes with lanthanide ions. Because of its cavity-like coordination structure and flexibility, L exhibits a stable conformation that provides a coordination cavity. It, therefore, shows high coordination ability and lipophilicity, both of which could make it a useful component sensor. Furthermore, it can be shown experimentally that the structures and properties of the amide-base tripod-type complexes are closely related to counter anion and terminal group effects [15–18]. A further study concerned with these will be reported in following communications.

4. Supplementary data

Crystallographic data for the structures reported in this paper have been deposited with the Cambridge Crystallographic data Center, CCDC no. 201065. Copies of this information may be obtained free of charge from the Director CCDC, 12 Union Road, Cambridge, CB2 1EZ, UK (Fax: +44-1223-336-033; E-mail: deposit@ccdc.cam.ac.uk or <http://www.ccdc.cam.ac.uk>).

Acknowledgements

We are grateful to the Foundation for University Key Teacher by the Ministry of Education, and the National Natural Science Foundation of China (projects 29571014 and 20071015) for financial support.

References

- [1] Y. Gao, J. Ni, J. Nucl. Radiochem. 5 (1982) 146.
- [2] J.C.G. Bunzli, J.M. Pfefferle, B. Ammann, G. Chapuis, F.J. Zuniga, Helv. Chim. Acta 67 (1984) 196.
- [3] L. Fan, W. Liu, X. Gan, N. Tang, M. Tan, W. Jiang, K. Yu, Polyhedron 19 (2000) 779.
- [4] W. Jiang, W. Liu, X. Li, Y. Wen, M. Tan, K. Yu, J. Mol. Struct. 611 (2002) 33–37.
- [5] I. Katsuki, Y. Motoda, Y. Sunatsuki, N. Matsumoto, J. Am. Chem. Soc. 124 (4) (2002) 629.

- [6] S. Franczyk, R. Czerwinski, *J. Am. Chem. Soc.* 114 (1992) 8138–8146.
- [7] T.M. Beasley, H.V. Lorz, *Technetium in the Environment*, 1986.
- [8] P.D. Beer, P.K. Hopkins, *Chem. Commun.* (1999) 1253–1254.
- [9] D. Li, X. Gan, M. Tan, X. Wang, *Polyhedron* 23 (1996) 3991.
- [10] G. Tan, J. Xu, F. Zhang, *Huaxue Shiji* 5 (1983) 100.
- [11] SHELXTL Version 5.10, Soft reference manual, Bruker Analytical X-ray System, Madison, Wisconsin, WI, 1997.
- [12] W.J. Greary, *Coord. Chem. Rev.* 7 (1971) 81.
- [13] S. Liu, W. Liu, M. Tan, K. Yu, *J. Coord. Chem.* 39 (1996) 105.
- [14] N.F. Curtis, Y.M. Curtis, *Inorg. Chem.* 4 (1965) 801.
- [15] G. Tan, T. Jiao, *Huaxue Tongbao* 9 (1987) 52.
- [16] Y. Hirashima, K. Kanetsuki, I. Yonezu, K. Kamakura, J. Shiokawa, *Bull. Chem. Soc. Jpn* 54 (1983) 738.
- [17] Y. Hirashima, K. Kanetsuki, I. Yonezu, K. Kamakura, J. Shiokawa, *Bull. Chem. Soc. Jpn* 54 (1981) 1576.
- [18] Y. Hirashima, K. Kanetsuki, I. Yonezu, K. Kamakura, J. Shiokawa, *Bull. Chem. Soc. Jpn* 54 (1986) 25.